X-622-67-49

NASA TM X-55705

SIMULTANEOUS CLOUD ALBEDO MEASUREMENTS TAKEN WITH AIRBORNE SOL-A-METERS AND, AIRBORNE AND NIMBUS II ORBITING MEDIUM RESOLUTION INFRARED RADIOMETER

A PRELIMINARY REPORT

BY

B.A. SPARKMAN

G.T. CHERRIX

FEBRUARY 1967

GODDARD SPACE FLIGHT CENTER

GREENBELT, MARYLAND

X-622-67-49

SIMULTANEOUS CLOUD ALBEDO MEASUREMENTS TAKEN WITH AIRBORNE SOL-A-METERS AND AIRBORNE AND NIMBUS II ORBITING MEDIUM RESOLUTION INFRARED RADIOMETER

A PRELIMINARY REPORT

by

B. A. Sparkman
and
G. T. Cherrix

Goddard Space Flight Center
Greenbelt, Maryland

CONTENTS

SIMULTANEOUS CLOUD ALBEDO MEASUREMENTS TAKEN WITH AIRBORNE SOL-A-METERS AND AIRBORNE AND NIMBUS II ORBITING MEDIUM RESOLUTION INFRARED RADIOMETER

by

B. A. Sparkman
and
G. T. Cherrix

ABSTRACT

Albedos of cloud, desert, and ocean surfaces were measured simultaneously with airborne Sol-A-Meters, two short-wave channels of an airborne Medium Resolution Infrared Radiometer (MRIR), and a single short-wave channel of the Nimbus II MRIR. Good agreement was found in coordinated measurements from all of the instruments.

SIMULTANEOUS CLOUD ALBEDO MEASUREMENTS TAKEN WITH AIRBORNE SOL-A-METERS AND AIRBORNE AND NIMBUS II ORBITING MEDIUM RESOLUTION INFRARED RADIOMETER

INTRODUCTION

Albedos measured by the Nimbus II Medium Resolution Infrared Radiometer (MRIR), inferred global albedos of ~20% when assuming isotropic reflectances. These values are much lower than those given by House[1], London[2], and others. The generally accepted global albedo is 35-40%.

To check the albedos measured by the Nimbus MRIR, a comparison to albedos obtained by an aircraft-borne MRIR and aircraft-borne Sol-A-Meters was made. The airborne MRIR and Sol-A-Meters were flown over the subsatellite track as Nimbus II passed overhead, thereby making simultaneous measurements of different target areas.

INSTRUMENT DESCRIPTIONS

A. Nimbus II MRIR*

The Nimbus II Medium Resolution Infrared Radiometer (MRIR) contains one channel, the 0.2 to 4 micron channel, (channel 5) which responds to short wave radiation. The Nimbus II User's Guide (July 1966), available from the Nimbus Project Office of the Goddard Space Flight Center, contains a complete description of this instrument. The basic MRIR is the same as the airborne MRIR which is described below.

B. Airborne MRIR

This instrument is an early Flight model (F-3) of the Nimbus type, 5 channel Medium Resolution Infrared Radiometer. Three of the channels (See Fig. 1) respond to radiation in the infrared region of the spectrum, (Channel 1, at 6.7 μ, 2 at 10μ to 11μ, and 4 at 5μ to 30μ). Channels 3 (0.55μ to 0.85μ) and 5 (0.2μ to 4μ) respond to short wave radiation. This experiment is concerned only with the measurements in the shortwave region.

*The term "Medium Resolution Infrared Radiometer" (MRIR) is actually a misnomer, since the satellite instrument contains a channel which responds in part to visible radiation (0.2μ to 4μ) and the airborne instrument contains two such channels (0.55μ to 0.85μ, and 0.2μ to 4μ). However, the term "MRIR" has been so widely adopted as to compel its use here.

Fig. 2 shows the MRIR without modifications for mounting on the aircraft. Fig. 3 is a diagram of the optical system of each channel. Only the filter (F) is different for these two channels. The scan mirror (M) is set at 45° to, and rotates about an axis parallel to the axes of the 5 cassagrainian telescopes such that each 50 by 50 milliradian field of view scans through a 360° arc in a plane perpendicular to the axis of rotation during its 7-1/2 second period. The airborne instrument scans in the vertical plane containing the longitudinal axis of the aircraft. The instrument was covered with a thick thermal foam jacket without obscuring the optics and scanning area. Heaters maintained the radiometer at 25°C. This assembly was shock mounted inside an aerodynamic fairing which was fastened to the underside of the aircraft's tail section. Fig. 4 shows the MRIR in the aerodynamic fairing mounted on the Convair 990 jet aircraft. A motor operated door was provided in the fairing for protection of the optics during take-off and landing. Fig. 5 represents the unobscured field of view of the short wave channels of the MRIR. Scanning is fore to aft in the downward viewing directions.

C. Airborne Sol-A-Meters

This instrument consists of two silicon (photo-voltaic solar cells. One mounted on the downward facing surface of the MRIR aerodynamic fairing, (See Fig. 4), and one mounted behind the aircraft vertical stabilizer on an upward facing platform. The cells are calibrated to indicate insolation over a full 2π steradian field of view within the spectral range from 0.35 to 1.15 microns. Fig. 6 gives the spectral response curve of a silicon solar cell. The ratio of the signal from the downward looking cell to that of the upward looking cell is used to calculate albedo.

METHOD OF MEASUREMENT

Since the airborne MRIR has a narrow view angle and scans from fore to aft in the direction of flight, its measurements yield values of bidirectional reflectance rather than albedo. In order to find albedo from these measurements they must first be converted to the energy reflected over a hemisphere. This is done by summing over all nadir angles θ, 0 to 90° and then over all azimuth angles, ψ, 0 to 360°. Fig. 7 shows these angles.

The effective energy reflected from a surface over a hemisphere, W, can be summed numerically by:

$$\overline{W} = \overline{H}^{*} \cos \zeta_0 \sum_{\phi=0}^{2\pi} \sum_{\theta=0}^{\pi/2} \rho(\theta\phi) \cos\theta \sin\theta \Delta\theta \Delta\phi \qquad (1)$$

where $\overline{H}^* \cos\zeta_0$ is the effective solar irradiance and ζ_0 is the solar zenith angle. $\overline{H}^*_\lambda$ is obtained by integrating the spectral solar irradiance, as given by Johnson[3], and the effective spectral response functions ϕ_λ of each channel over all wavelengths. That is:

$$\overline{H}^* = \int_{\lambda=0}^{\infty} H^*_\lambda \, \phi_\lambda \, d\lambda . \tag{2}$$

The bidirectional reflectance, $\rho(\theta\phi)$ is a function of azimuth and nadir angle, and is defined by:

$$\rho(\theta\phi) = \frac{\overline{N}}{\overline{H}^* \cos \zeta_0} \tag{3}$$

where $\overline{N}$ is the effective reflected radiance.

Albedo, by definition, is the ratio of the amount of radiation reflected by a body to the amount incident upon it. Therefore, Albedo, A, is given by

$$A = \frac{\overline{W}}{\overline{H}^* \cos \zeta_0} \tag{4}$$

Thus the albedo in terms of bidirectional reflectance is:

$$A = \sum_j \sum_i \rho(\theta\phi) \cos\theta \sin\theta \, [\Delta\theta]_i \, [\Delta\phi]_j \tag{5}$$

To choose the corresponding reflectance measurements from the Nimbus II MRIR, Advanced Vidicon Camera System (AVCS) photos of the target area were used to select the best location for readout. Figs. 8 through 11 show aircraft locations and satellite scan spots (resolution areas of the satellite MRIR) for each target area. The target directly below the aircraft position, in most cases, did not uniformly fill the field of view of the satellite instrument. Therefore, a scan spot was selected near the aircraft position in which the target did fill the field of view of the satellite-borne MRIR.

DATA

Measurements were made simultaneously with the Nimbus II MRIR over the Pacific Ocean, Salt Lake Desert, and stratocumulus clouds. Bidirectional reflectance measurements were taken with 0 to 90° nadir angles in the principal plane of the sun, (with solar azimuth angles of both 0 and 180°). An azimuth angle of 0° is identified with the direction of forward scatter, and 180° is identified with the direction of backscatter). (See Fig. 7).

These values were summed using Eq. (5) to find albedo at 5° nadir angle intervals, and 180° azimuth angle intervals. That is, the bidirection reflectances measured for 0° azimuth were taken to be constant from 90° through 180° to 90° azimuth.

It is possible to make this summation because measurements were made near local noon, when the sun is high in the sky and reflectances from cloud and ground surfaces are nearly isotropic. It must be emphasized here that this type of summation is only valid for very small solar zenith angles. As the solar zenith increases, reflectances become increasingly anisotropic with the maximum energy scattered in the forward direction. With these larger zenith angles, the summation must be properly weighted to account for this anisotropy.

RESULTS AND CONCLUSIONS

Results of four simultaneous measurements are shown in Table 1. Albedos inferred from the airborne Sol-A-Meters and MRIR are compared to reflectance measurements from the Nimbus II MRIR. There is very good agreement between the three instruments for each target case. In case 1, the higher reflectance measured by the Nimbus II MRIR can be attributed to the thin cirrus clouds above the aircraft.

This preliminary comparison of the aircraft and Nimbus II data indicates that the Nimbus II reflectances are, indeed, correct.

ACKNOWLEDGMENTS

We would like to thank Dr. Nordberg for initiating this report. We appreciated the cooperation of the Nimbus Project Office for supplying the AVCS photos and the satellite MRIR data.

REFERENCES

1. House, F. B., "The Radiation Balance of the Earth From a Satellite," Ph. D. Dissertation, Univ. of Wisconsin, Dept. of Meteorology, 1965.

2. London, J., "A Study of the Atmospheric Heat Balance," Final Report, Contract No. AF 19 (122) – 165, Research Division College of Engineering, New York, University.

3. Johnson, F. S., Ed., "Satellite Environment Handbook," (Stanford University Press, Stanford, Calif., 1961).

BIBLIOGRAPHY

Coulsen, K. L., G. M. Bauricius and E. L. Gray, "Effects of Surface Reflection on Radiation Emerging From the Top of a Planetary Atmosphere," Report NASA Contr. No. NAS5-3925, Sept. 1965.

Bartman, F. L., "The Reflectance and Scattering of Solar Radiation by the Earth," Preliminary Report NASA Contr. NASr-54(03), Feb. 1967.

Deirmendjian, D., "Scattering and Polarization of Water Clouds and Haze in the Visible and Infrared," Appl. Opt. 3, 187 (1964).

Bauer, E., "The Scattering of Infrared Radiation from Clouds," Appl. Opt. 3, 197 (1964).

Bandeen, W. R., M. Halev and I, Strange, "A Radiation Climatology in the Visible and Infrared From the TIROS Meteorological Satellite", NASA TN D-2534, National Aeronautics and Space Administration, Washington, D. C., June 1965.

House, F. B., "The Radiation Balance of the Earth From a Satellite," Ph. D. Dissertation, Univ. of Wisconsin, Dept. of Meteorology, 1965.

Aldrich, L. B., "The Reflecting Power of Clouds," Smithsonian Misc. Coll., 69, No. 10, (1919).

Luckiesh, M., "Aerial Photometry," Astrophys. Jour., Vol. 49, pp. 108-130, (1919).

Neiburger, M., "Reflection Absorption and Transmission of Insolation by Stratus Clouds," J. Meteor., Vol. 6, pp. 98-104, (1919).

Kondratiev, K. Y., Z. F. Mironova, and A. N. Otto, "Spectral Albedo of Natural Surfaces," Pure and Applied Geophysics, Vol. 59, No. 3, pp. 207-216 (1964).

Coulsen, K. L., G. M. Bouricius and E. L. Gray, "Optical Reflection Properties of Natural Surfaces," J. Geophys. Res., 70(18), 4601-4611, 1965.

Bauer, K. G., and J. A. Dutton, "Albedo Variations Measured from an Airplane Over Several Types of Surfaces," J. Geophys. Res. 67(6), 2367-2376, 1962.

Marlatt, W. E., "Investigations of the Temperature and Spectral Emissivity Characteristics of Cloud Tops and of the Earth Surface," Report NASA Contr. No. NASr-147, Feb. 1964.

Van de Hulst, N. C., "Light Scattering by Small Particles," J. Wiley and Sons, Inc., New York, 1957.

Blau, Henry H., Jr., Ronald P. Espinola and Edward C. Rufenstein, III, "Near Infrared Scattering by Sunlit Terrestrial Clouds," Appl. Opt. 5, 555, (1966).

London, J., "A Study of the Atmospheric Heat Balance," Final Report, Contr. No. A. F. 19(122) - 165, Research Division College of Engineering, New York University.

Bartley, C. E., "Theoretical Estimates of Cloud Reflection and Transmission in the Infrared," Appl. Opt. 4, 847, 1965.

Johnston, F. S., Ed., "Satellite Environment Handbook; (Stanford University Press, Stanford, Calif., 1961).

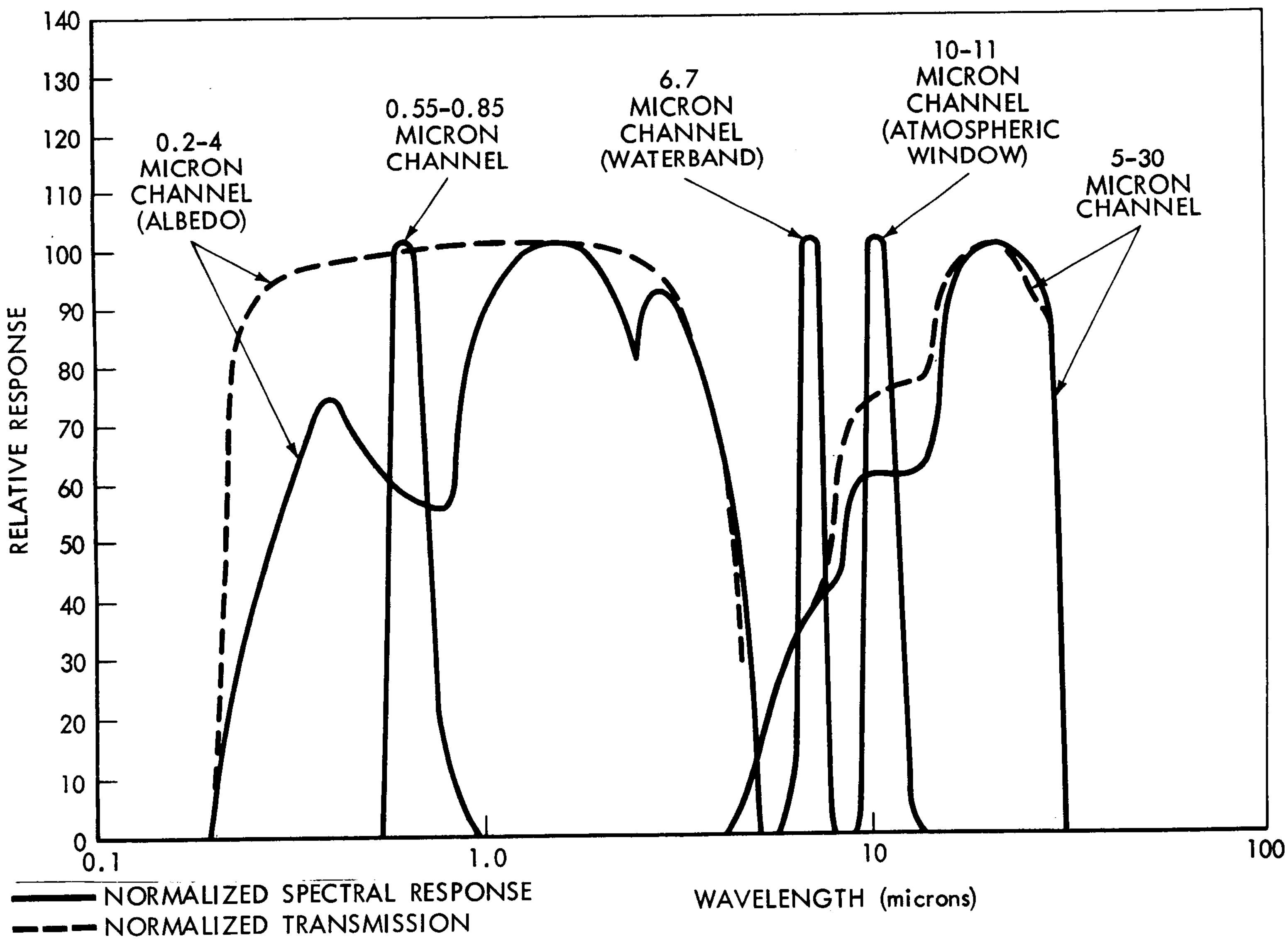

Figure 1—Filter and Relative Spectral Response of Nimbus Five-Channel Radiometer

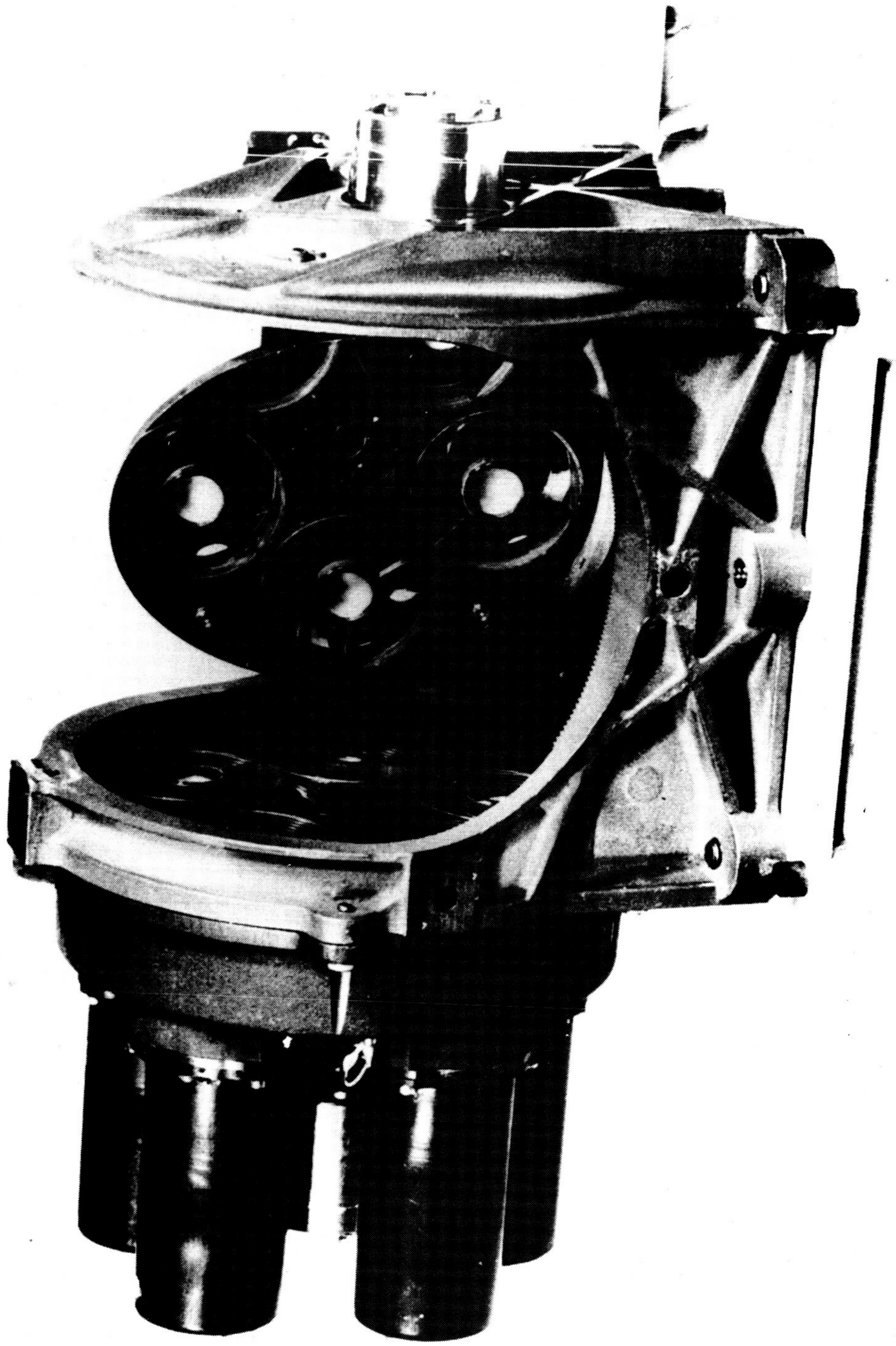

Figure 2—Medium Resolution Infrared Radiometer, (MRIR)

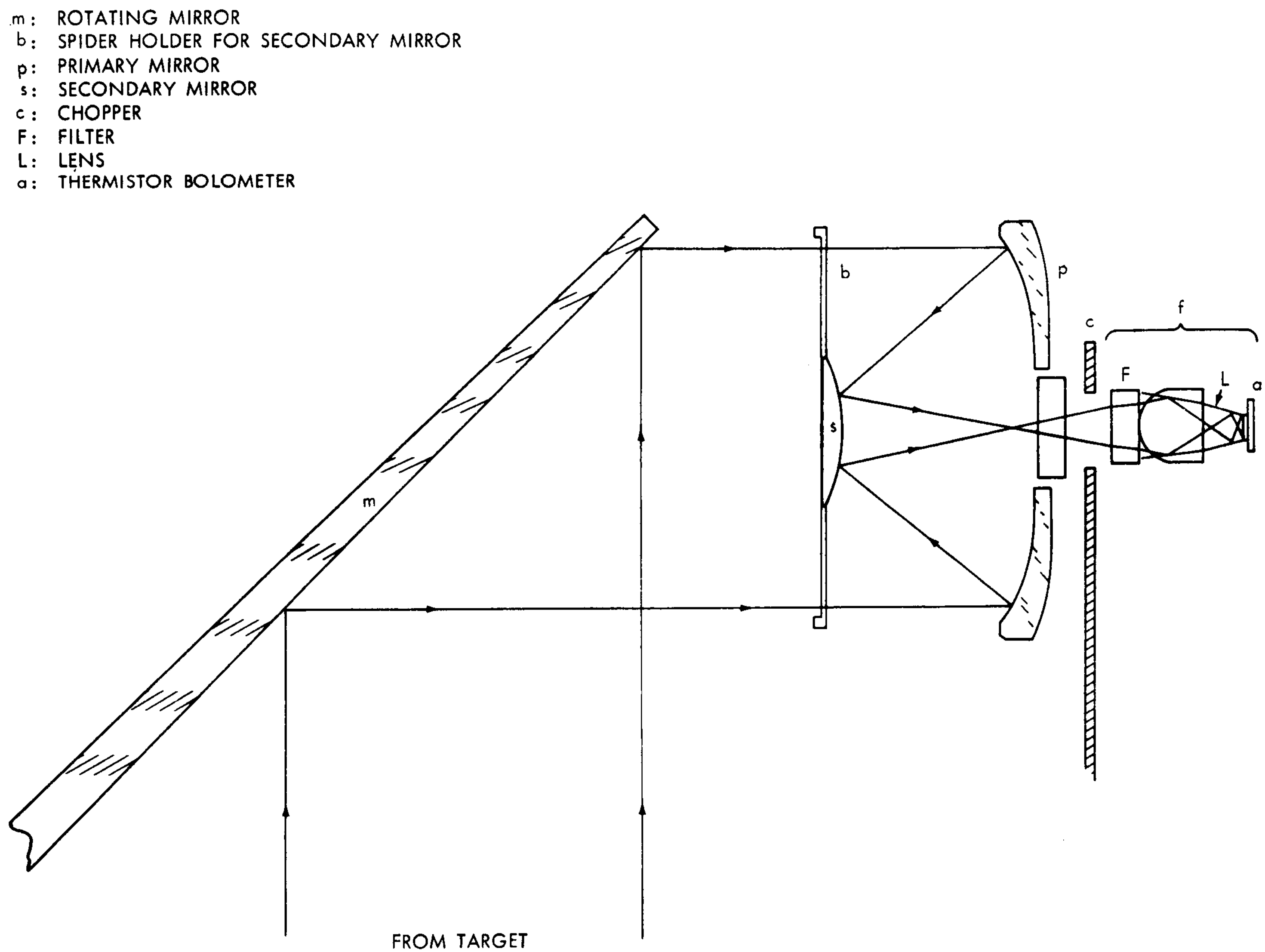

Figure 3–Optical System of the MRIR

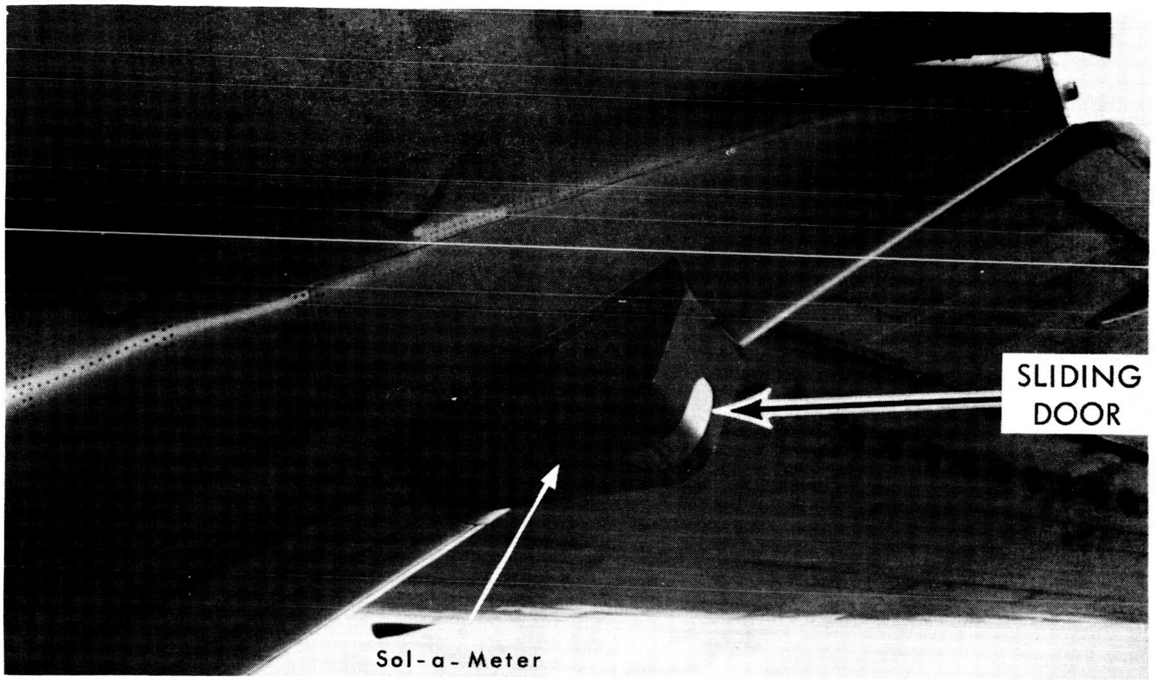

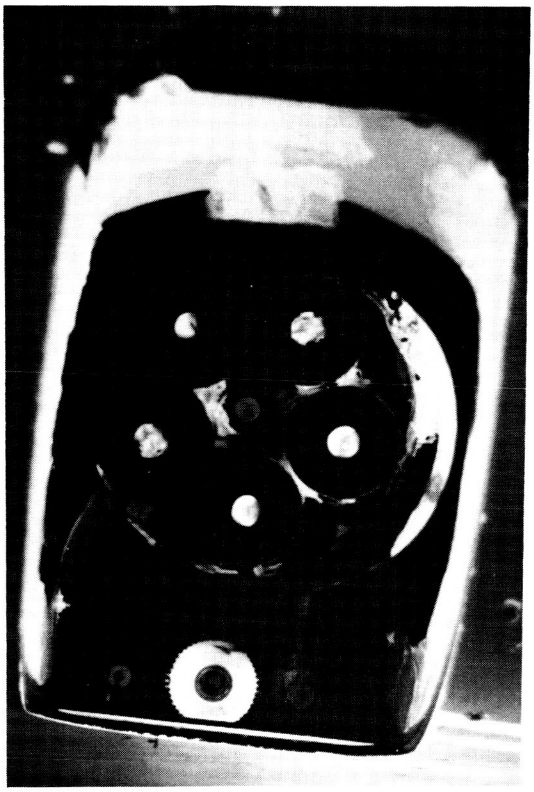

Figure 4—MRIR and Sol-A-Meter Mounted in Aircraft Fairing

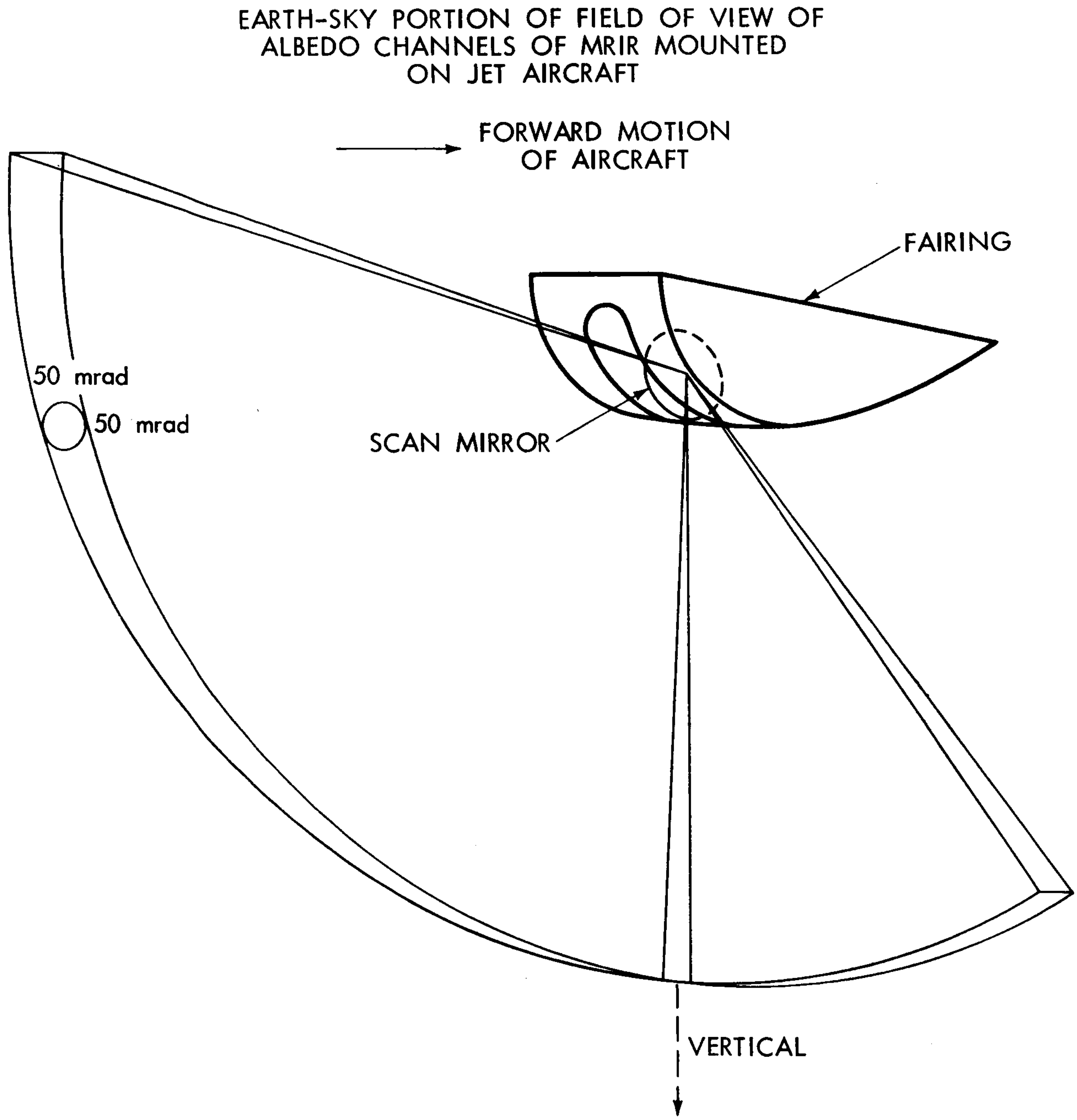

Figure 5—Earth-Sky Portion of View of Albedo Channels of MRIR

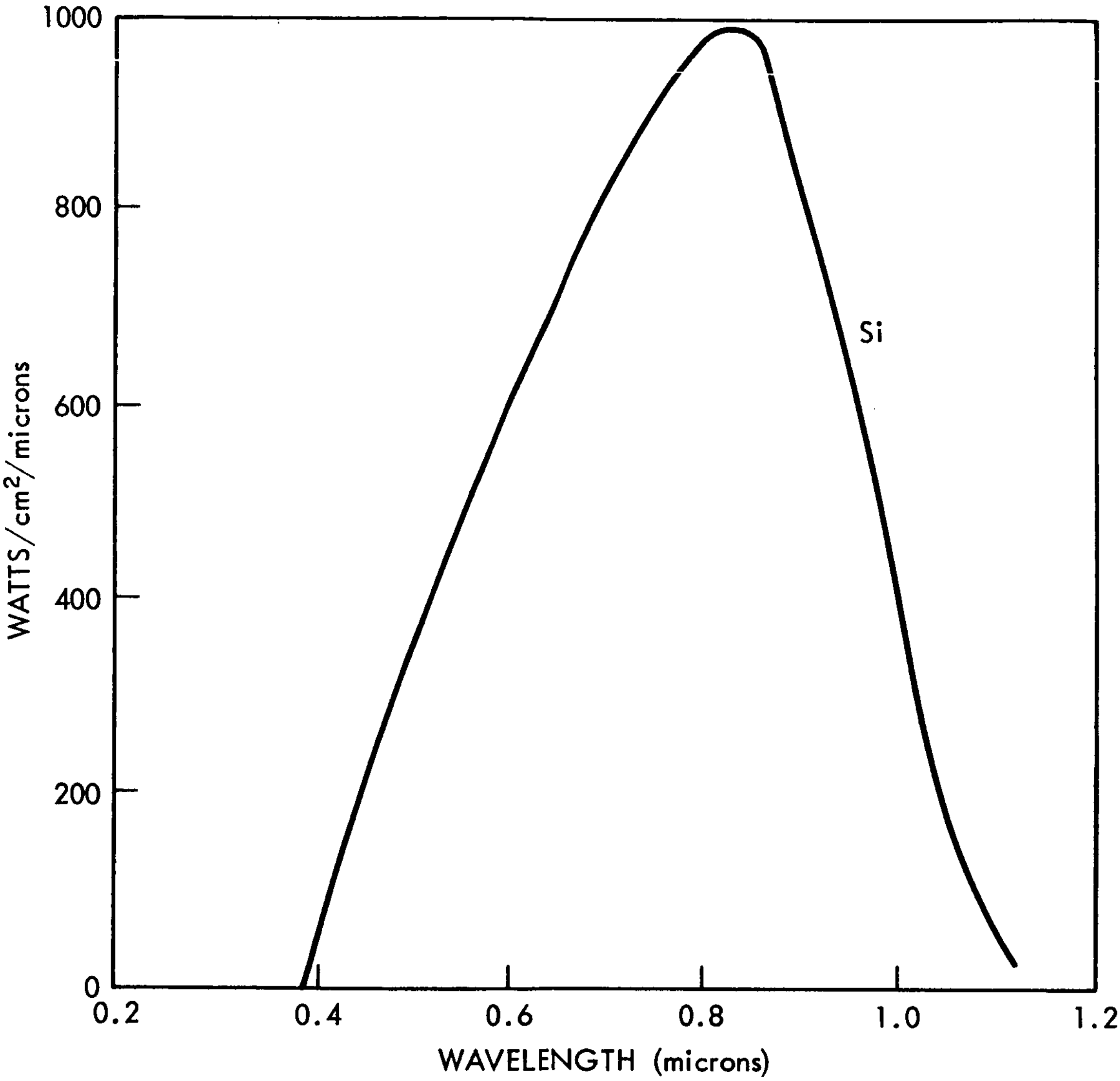

SILICON CELL SPECTRAL RESPONSE

Figure 6–Spectral Response of a Silicon Solar Cell

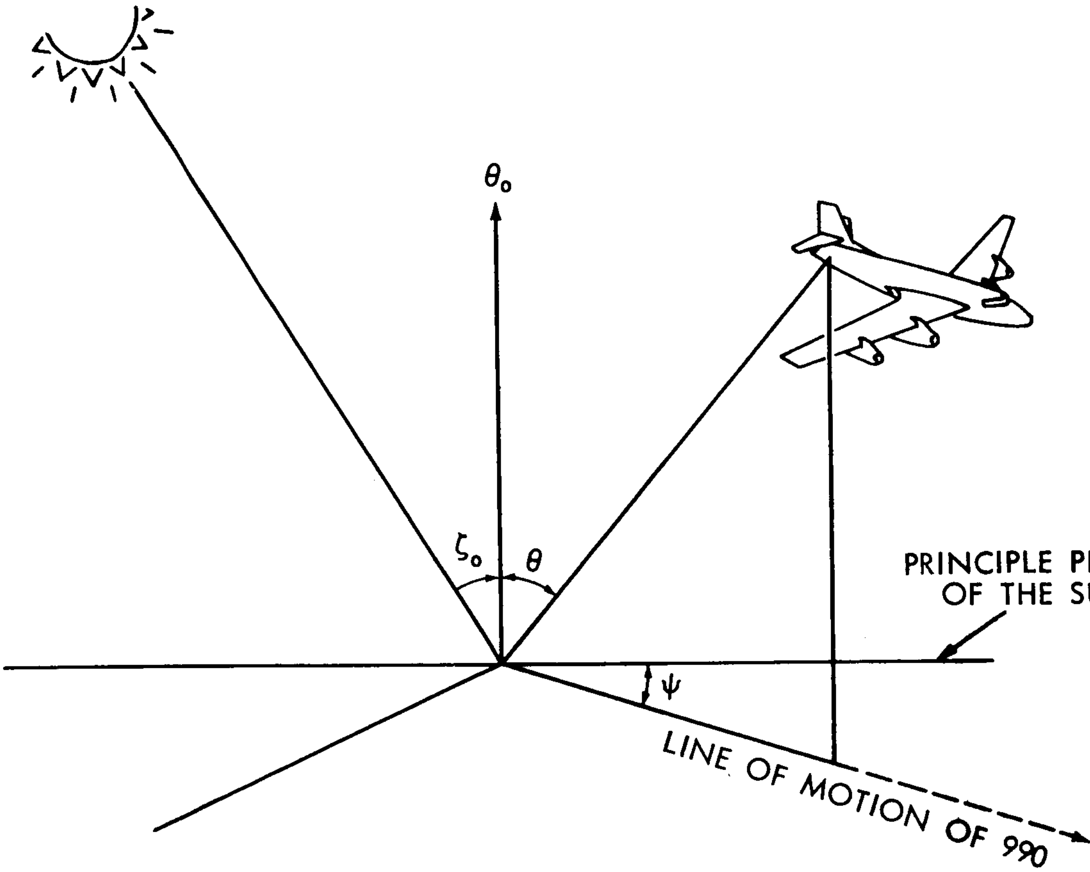

ζ_o = SOLAR ZENITH ANGLE

θ = NADIR ANGLE OF REFLECTED ENERGY

ψ = HORIZONTAL ANGULAR DEPARTURE OF 990'S FLIGHT PATH OUT OF THE PRINCIPAL PLANE OF THE SUN

θ_o = LOCAL VERTICAL

Figure 7–Diagram Showing Solar Zenith, Azimuth, and Nadir Angles

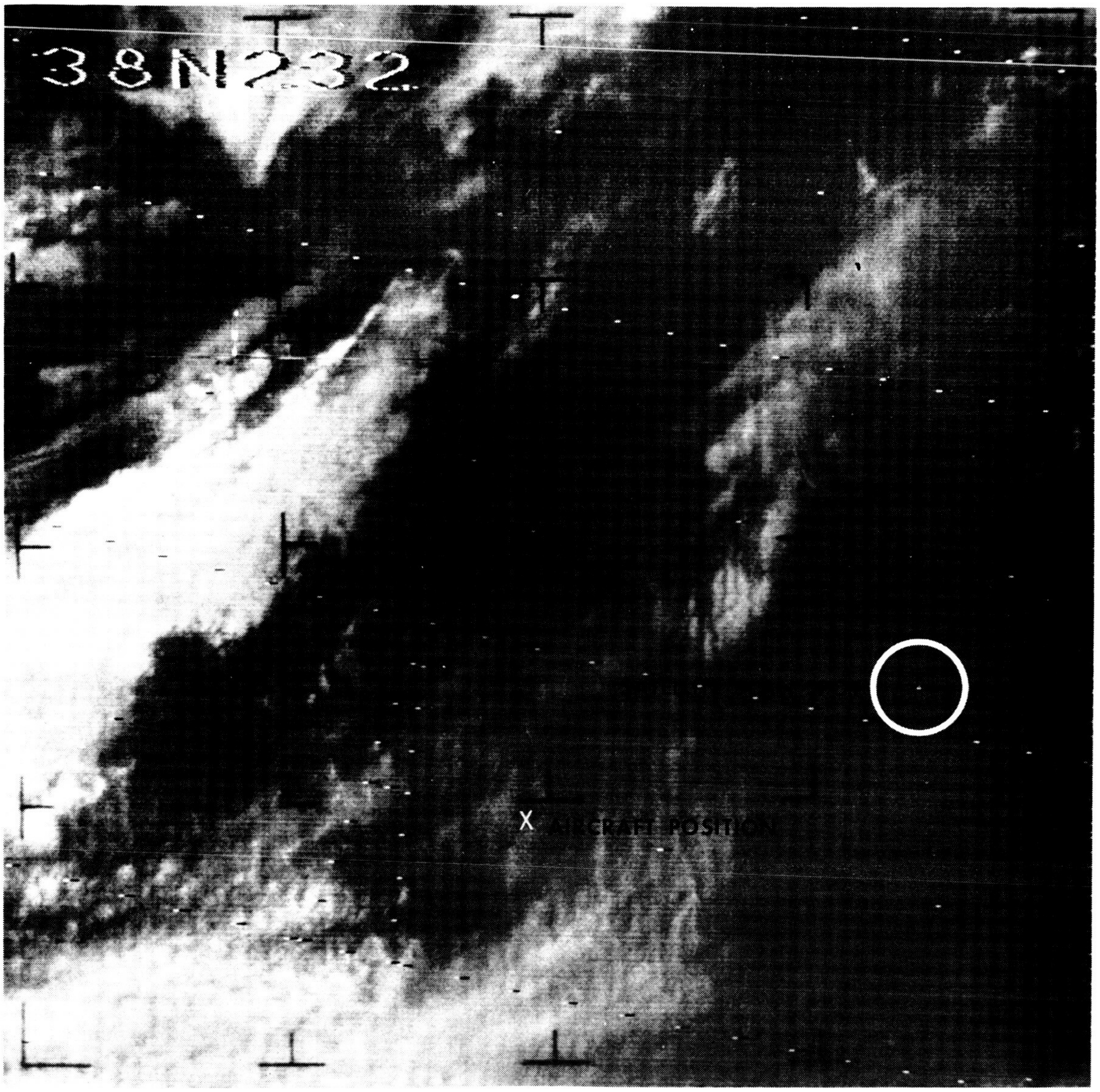

Figure 8—Clear Pacific Ocean with Scattered Cirrus Clouds Above Aircraft

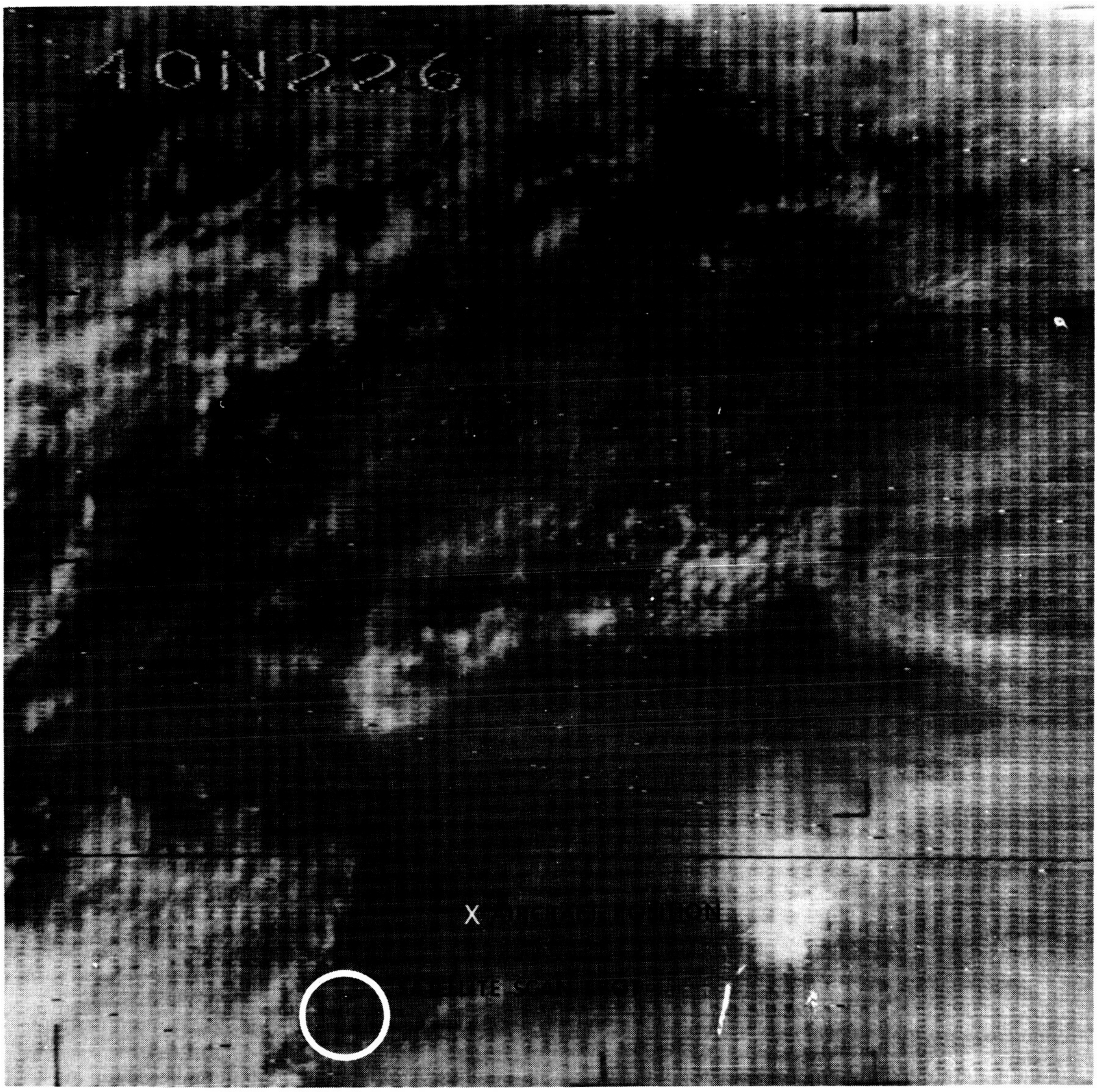

Figure 9—Broken Stratocumulus Clouds Over Pacific Ocean Near Coast of California

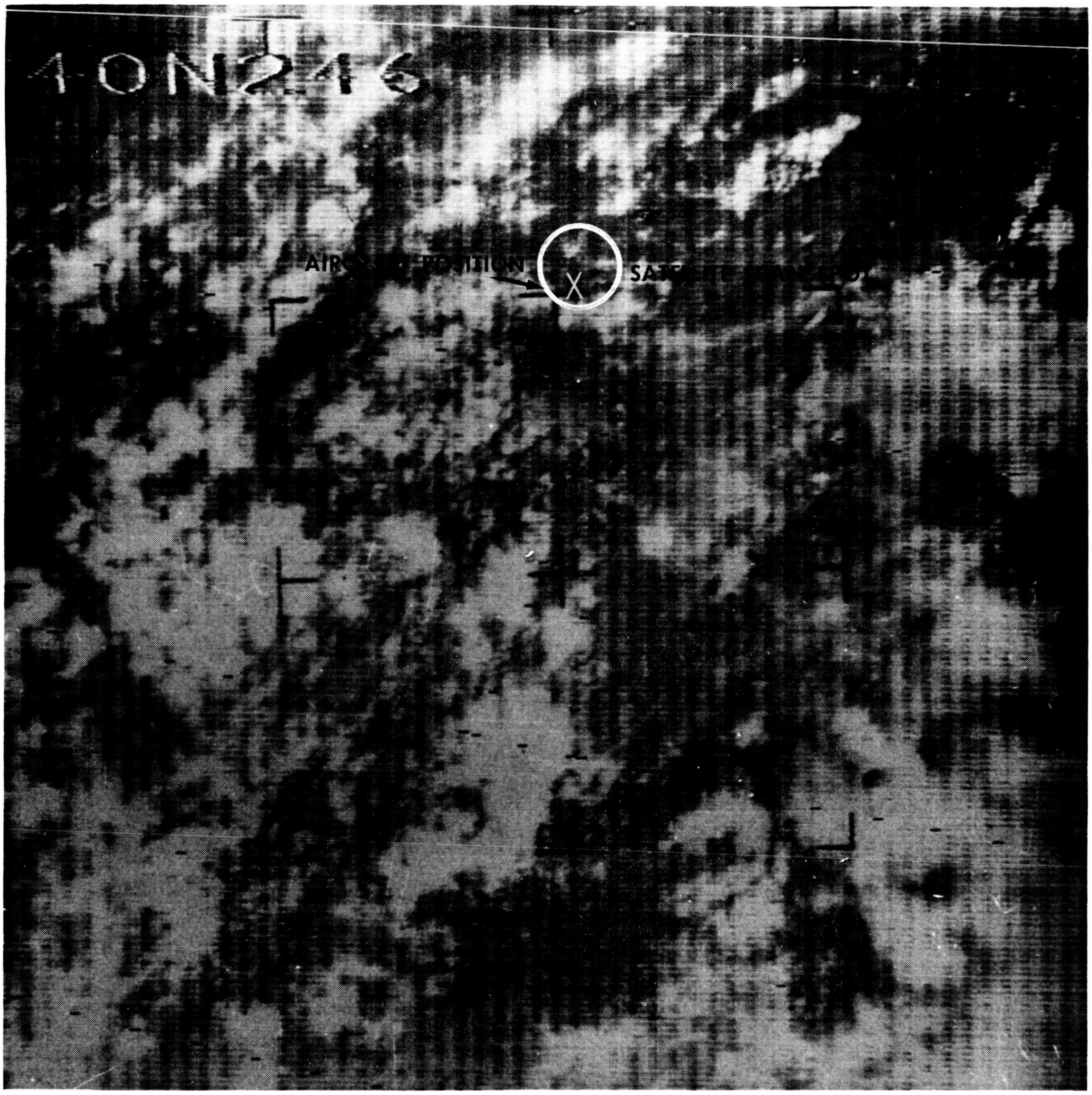

Figure 10–Salt Lake Desert, Utah

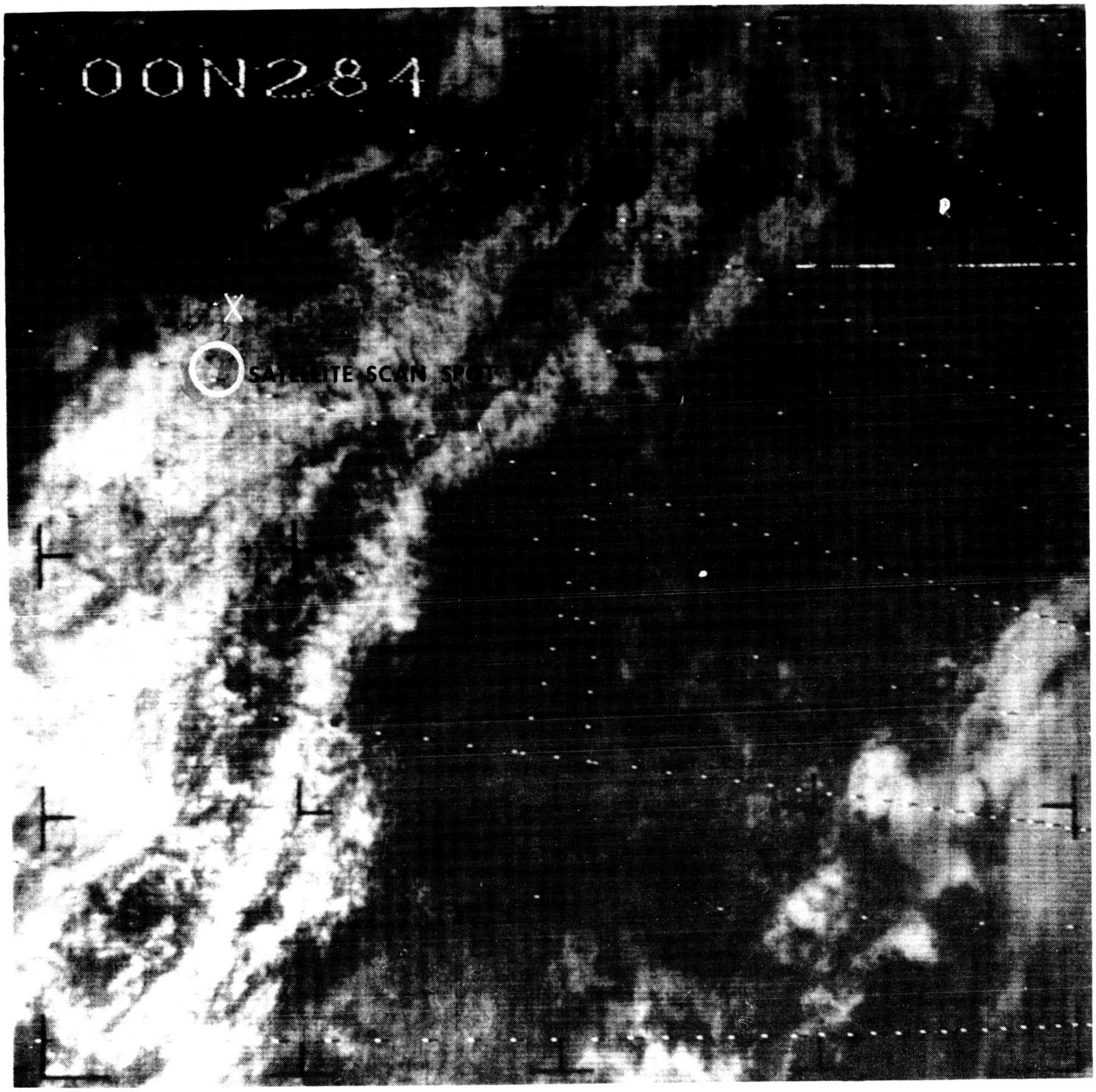

Figure 11–Stratocumulus Clouds Over Esmeraldes, Equador

Table 1

Convair 990 MRIR Reflectance Measurements to Correlate With Nimbus II Reflectance Measurements

Case	Target	Nimbus Orbit	Date	Time U.T.	Lad. °N	Long. °W	Azimuth Heading To Sun	Albedo CH_3	Albedo CH_5	Reflectance Nimbus II	Albedo Sol-A-Meters
1	Clear to Pacific Ocean, Some Ci Above	446	6-17-66	2000	37	127	0 & 180	4.71	5.37%	7.05%	4.87%
2	Broken Strato Cu Over Pacific	393	6-13-66	2003	37	134°39'	0 & 180	19.15	19.2	20.05	19.28
3	Salt Lake Desert	339	6-9-66	1833	40°45'	114°09'	0 & 180	34.2	31.39	32.36	37.21
4	Strato Cu Over Esmeraides	112	5-23-66	1712	00°55'	79°38'	180	55.99	45.21	41.25	56.07